

Comparative Evaluation of the Cerebral and Cerebellar White Matter Development in Pediatric Age Group using Quantitative Diffusion Tensor Imaging

Sona Saksena · Nuzhat Husain · Gyanendra K. Malik ·
Richa Trivedi · Manoj Sarma · Ramkishore S. Rathore ·
Chandra M. Pandey · Rakesh K. Gupta

Published online: 26 June 2008
© Springer Science + Business Media, LLC 2008

Abstract Age-dependent changes in the normal cerebral white matter have been reported; however, there is no study on normal cerebellar white matter maturation in developing brain using diffusion tensor imaging (DTI). We performed DTI in 21 children who had normal neurological assessment along with no evidence of any abnormality on imaging. The aim of this study was to compare the age-related changes in fractional anisotropy (FA) and mean diffusivity (MD) quantified from cerebral white matter (splenium and genu of the corpus callosum and posterior limb of the internal capsule) and cerebellar white matter (middle cerebellar peduncles, superior cerebellar peduncles,

and inferior cerebellar peduncles) regions in healthy children ranging in age from birth to 132 months. Log-linear regression model showed best fit to describe the age-related changes in FA and MD both for cerebral and cerebellar white matter. In cerebral white matter, an initial sharp increase in FA was observed up to the age of 24 months followed by a gradual increase up to 132 months. In cerebellar white matter, sharp increase in FA was observed up to 36 months, which then followed a gradual increase. However, MD showed a sharp decrease in cerebral white matter up to 24 months followed by a more gradual decrease thereafter, while in cerebellar white matter after an initial decrease (6 months), it followed a stable pattern. This study provides normative database of brain white matter development from neonates to childhood. This quantitative information may be useful for assessing brain maturation in patients with developmental delay of the cerebral and cerebellar white matter.

S. Saksena · R. Trivedi · R. K. Gupta (✉)
Department of Radiodiagnosis,
Sanjay Gandhi Post Graduate Institute of Medical Sciences,
Raebareilly Road,
Lucknow, Uttar Pradesh 226014, India
e-mail: rgupta@sgpgi.ac.in

N. Husain
Department of Pathology, Chatrapati Shahuji Maharaj University,
Lucknow, Uttar Pradesh, India

G. K. Malik
Department of Pediatrics, Chatrapati Shahuji Maharaj University,
Lucknow, Uttar Pradesh, India

M. Sarma · R. S. Rathore
Department of Mathematics and Statistics,
Indian Institute of Technology,
Kanpur, Uttar Pradesh, India

C. M. Pandey
Department of Biostatistics,
Sanjay Gandhi Post Graduate Institute of Medical Sciences,
Lucknow, Uttar Pradesh, India

Keywords White matter development · Myelination ·
Fractional anisotropy · Mean diffusivity

Introduction

The human brain undergoes an extended period of postnatal maturation. Myelination of white matter is one of the main processes of brain development that proceeds systematically throughout the postnatal phase and continues into adulthood [1–4]. This process is essential for the rapid development of motor learning and cognitive functions [5, 6]. Furthermore, the understanding of the developing human brain is of great clinical importance, as many

neurological and neurobehavioral disorders originate during this process of development. Though the histological studies have shown changes in the developing human brain [7–9], these are unable to provide sequential information related to its development as the technique is invasive.

White matter myelination in infants and children can be assessed noninvasively using magnetic resonance imaging (MRI) [10–12]. During the process of development, brain undergoes considerable anatomical changes that affect the relaxation property of the MR parameters. It has been reported that the T1 and T2 relaxation times become shorter as the myelination progresses [10, 11]. However, conventional MRI has several limitations in the evaluation of brain development [13].

Diffusion-weighted imaging has demonstrated early changes in apparent diffusion coefficient (ADC) and anisotropy in white matter tracts even before the onset of myelination histologically or on T1- and T2-weighted imaging [14, 15]. Nomura et al. [16] reported decreased ADC and increased white matter anisotropy during the first 6 months of postnatal life. Morriss et al. [17] demonstrated decreased ADC and increased anisotropy during the first 3 years of postnatal life in major white matter tracts in 30 children aged 1 day to 17 years. Fluid-attenuated inversion recovery (FLAIR) imaging has been also used to investigate the normal appearance of white matter myelination in infants and children [18, 19]. Magnetization transfer (MT) imaging has shown age-dependent changes in MT ratios of white matter in normal children [20, 21].

Diffusion tensor imaging (DTI) has provided quantitative assessment of the water diffusion in tissues at the microstructural level. The diffusion of water in white matter is anisotropic due to the presence of myelin sheath [22]. The commonly used DTI metrics are mean diffusivity (MD), which measures the magnitude of diffusion, and fractional anisotropy (FA), which quantifies the preferential direction of water diffusion along white matter tracts. The first investigations of human brain maturation with DTI were performed on preterm and term neonates, and showed that the isotropic diffusion coefficient decreases and diffusion anisotropy rises with increasing gestational age [23–25]. Other authors extended these observations to normal brain development in infants and children, showing strong positive correlation between anisotropy and age, and negative correlation between overall diffusion and age in major white matter tracts [26–29]. These results are consistent with ongoing myelination and decreased water content with age.

In most of the DTI studies, age-dependent changes in the normal cerebral white matter have been reported [26–29]. In a recent study, Dubois et al. [30] did not find any

significant age-related changes in FA, while significantly decreased MD values were observed in middle cerebellar peduncles (MCP) of healthy infants ranging from 1 to 4 months. However, a detailed study of normal cerebellar white matter maturation in developing brain with DTI has not yet been performed.

The current study was performed with the aim to compare age-related changes in DTI metrics (FA and MD) quantified from cerebral white matter [splenium and genu of corpus callosum, and posterior limb of the internal capsule (PLIC)] and cerebellar white matter [MCP, superior cerebellar peduncles (SCP), and inferior cerebellar peduncles (ICP)] regions in healthy children ranging in age from birth (0.2 months) to 132 months.

Materials and Methods

Twenty-one children (mean age, 38.40 months; range, 0.2–132 months) were included in the study. These children were attending the Department of Pediatrics, Chatrapati Shahuji Maharaj Medical University, Lucknow, for complaints of isolated mild peripheral joint injury. There were six children aged 0.2–3.5 months (term babies), three 8–12 months, four 15–24 months, and eight 48–132 months. Additional brain imaging was also performed in these children. The inclusion criteria were (1) normal neurological assessment and (2) clinical brain imaging study showing no visible abnormality. Children with a known brain disorder or with specific clinical evidence of neurological dysfunction were excluded from this study. All studies were performed within the guidelines of the Institutional Ethics Committee. Informed consent was obtained from the parents of all the children after explaining the purpose of the study.

MRI Protocol

Imaging Parameters

Imaging was performed on a 1.5-T MRI scanner (Signa Lx Echo speed plus, General Electric Healthcare Technologies, Milwaukee, WI, USA) using a standard birdcage receive and transmit radiofrequency quadrature knee coil (neonates up to 1 month) and head coil (infants, 1–12 months; children, 12–132 months). The gradient system was capable of *delivering* maximal gradient amplitude of 33 mT/m. MR imaging parameters included T2-weighted axial fast spin-echo images using repetition time (TR)=6,000 ms, echo time (TE)=85 ms, number of excitation (NEX)=4, T1-weighted axial spin-echo (SE) images with TR=1,000 ms,

TE=14 ms, NEX=2, and T1 FLAIR images with TR=2,250 ms, TE=9.0, inversion time=600 ms, NEX=4. A total of 36 contiguous 3-mm-thick axial sections were acquired with a 240×240 mm field of view (FOV) and image matrix of 256×256.

DTI Protocol

DTI data were acquired using a single-shot echo-planar dual SE sequence with ramp sampling [31]. The diffusion-weighted acquisition parameters were b -factor=0 s/mm², 700 s/mm² (neonates up to 1 month and infants from 1 to 12 months), 1,000 s/mm² (children, 12–132 months), slice thickness=3 mm with no gap, number of slices=34–36, FOV=240×240 mm, TR=8 s, TE=100 ms, and NEX=8. The acquisition matrix was 128×80, and the homodyne algorithm was used to construct the k -space data to 128×128 and zero-filled to generate an image matrix of 256×256. The diffusion tensor encoding used was the balanced rotationally invariant [32] dodecahedral scheme with ten uniformly distributed directions over the unit hemisphere. DTI imaging was completed in 9.36 min.

DTI Data Processing and Analysis

The magnitude averaged data were transferred to a workstation for further analysis. DTI data analysis involves three major steps: pre-processing, processing, and post-processing.

Data Pre-Processing

The data were distortion-corrected for shear, scale, rotation, and translation using the Automated Image and Registration package [33]. The removal of scalp to isolate the brain in the collected raw images was done in all the cases by an automated stripping procedure [34]. Subsequent DTI processing did not require any filtering, as justified by the absence of unprocessed voxels.

Data Processing

The distortion corrected data were then interpolated to attain isotropic voxels and decoded to obtain the tensor field for each voxel. The tensor field data were then diagonalized using the analytical diagonalization method [35] to obtain the eigenvalues (λ_1 , λ_2 , and λ_3) and the three orthonormal eigenvectors (e_1 , e_2 , and e_3). The orthogonality of the computed eigenvectors and the correctness of the eigenvalues were checked using random sampling at a number of voxels. The correctness observed was up to an order of 10^{-17} , indicating that no iterative refinement of the computed eigenvalues/vectors was needed. The tensor field

data was then used to compute the DTI metrics such as mean diffusivity (Eq. 1.0) and fractional anisotropy (Eq. 2.0) for each voxel.

$$MD = \frac{\lambda_1 + \lambda_2 + \lambda_3}{3} \quad (1.0)$$

$$FA(\lambda_1, \lambda_2, \lambda_3) = \frac{1}{\sqrt{2}} \sqrt{\frac{(\lambda_1 - \lambda_2)^2 + (\lambda_2 - \lambda_3)^2 + (\lambda_1 - \lambda_3)^2}{\lambda_1^2 + \lambda_2^2 + \lambda_3^2}} \quad (2.0)$$

Data Post-Processing and Quantification

Analysis of the conventional as well as DTI images was undertaken by an experienced neuroradiologist (R.K.G.). Java-based software was used to calculate various DTI-derived metrics (FA and MD) [36]. The DTI-derived maps were displayed and overlaid on images with different contrasts to facilitate the region-of-interest (ROI) placement. For FA and MD quantification, ROIs were placed on the corpus callosum, internal capsule, and cerebellar peduncles. Elliptical and/or rectangular ROIs were placed at the level of third ventricle to obtain FA and MD values in genu and splenium of corpus callosum and PLIC (Fig. 1). We defined the levels of MCP, SCP, and ICP on the basis of the anatomic landmarks visible on DTI color maps as described in detail elsewhere [37]. Elliptical ROIs were placed at the level of pons in the axial plane for MCP, while for SCP and ICP, a coronal plane passing obliquely through it was selected for the placement of ROIs (Fig. 1). The size of the ROI varied from 2×2 and 6×6 pixels (minimum number = 4 pixels and maximum number = 36 pixels).

Statistical Analysis

Linear, quadratic, cubic, log-linear, growth, and exponential models were used to explain the relationship between age and DTI indices (FA and MD). For each model regression coefficients, R^2 and 95% confidence interval of the mean were estimated. The computations were performed using the statistical package for social sciences (SPSS, V15, Inc., Chicago, IL, USA). Based on regression diagnostics, the log-linear model given below (Eq. 3.0) was found to have a best fit, and the results of this analysis were used to explain various relationships. p value less than or equal to 0.05 was considered to be significant.

$$y = b_1 \ln(x) + b_0 \quad (3.0)$$

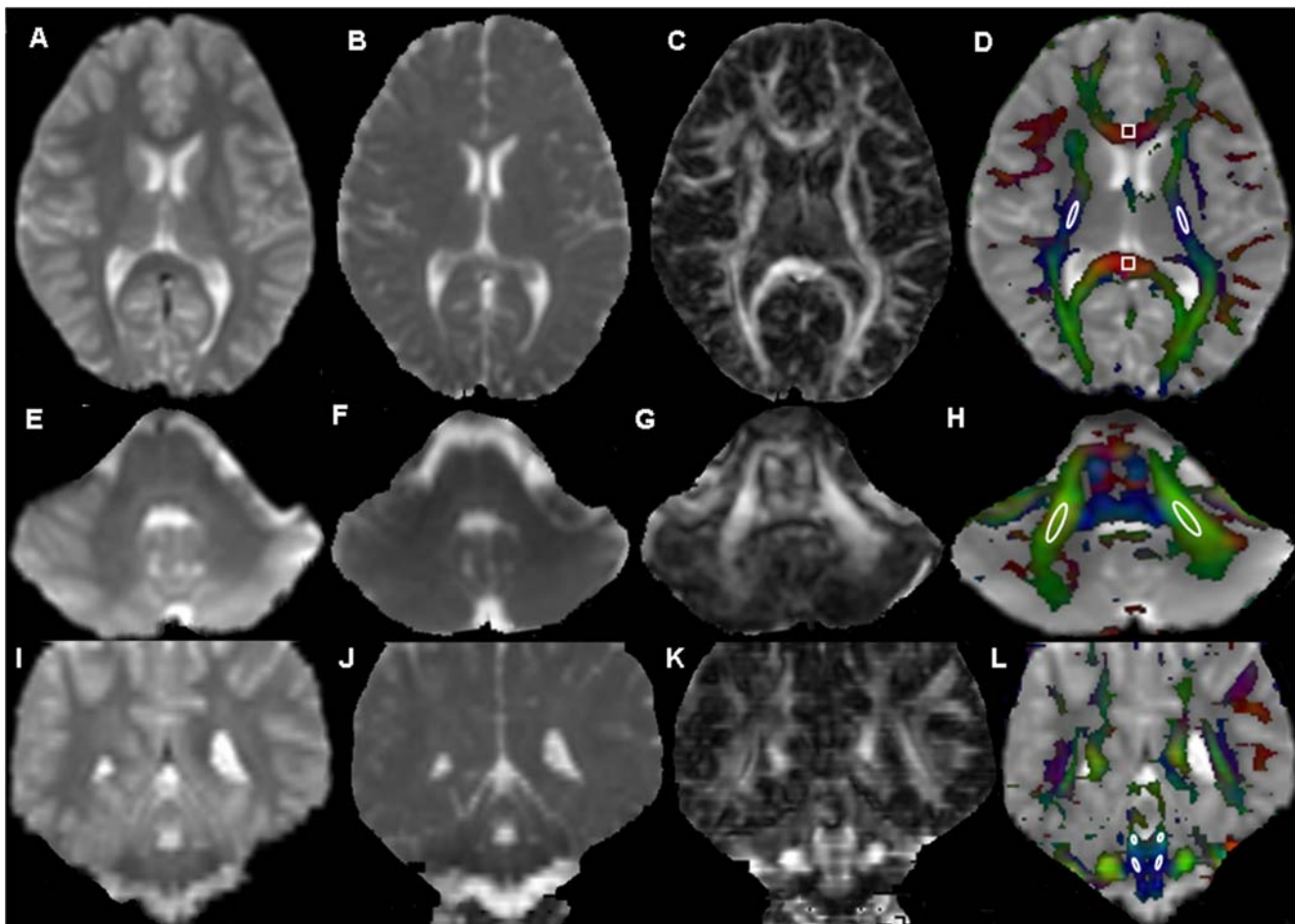


Fig. 1. Axial and coronal images in an 8-year-old child showing normal cerebral and cerebellar white matter. T2-weighted image, mean diffusivity, fractional anisotropy (FA), and color-coded FA maps at the level of third ventricle (**a–d**), pons (**e–h**), and fourth ventricle (**i–l**) showing region-of-interest(s) placed on color-coded FA maps on the genu and splenium of the corpus callosum, posterior limb of the

internal capsule, middle cerebellar peduncles, superior cerebellar peduncles, and inferior cerebellar peduncles, respectively. The cut off value for the color-coded FA map for display is kept at 0.2, above which the color-coded regions reflect the white matter only [red (right–left), green (anterior–posterior), and blue (superior–inferior)]

where y is the estimated DTI value, x is the age, b_0 is the constant term, and b_1 is the regression coefficient of the log transform of age.

Results

FA and MD Values

The mean FA values for all age groups was found to be highest in splenium (0.48 ± 0.04) followed by the genu (0.47 ± 0.04) of the corpus callosum, MCP (0.45 ± 0.06), PLIC (0.38 ± 0.03), SCP (0.35 ± 0.06), and ICP (0.34 ± 0.05 ; Table 1). The mean MD values was highest in the genu of the corpus callosum (1.09 ± 0.22) followed by PLIC (1.00 ± 0.19), splenium of the corpus callosum (1.00 ± 0.16), ICP (0.71 ± 0.05), SCP (0.67 ± 0.03), and MCP (0.66 ± 0.03) for all age groups (Table 2).

Log-Linear Graphs

The FA was lowest in newborns, while it was highest in children for all the ROIs placed on different cerebral and cerebellar white matter regions. The MD for these ROIs followed an opposite trend being highest in newborns and lowest in children. In all ROIs, the FA increased, while MD decreased continuously (Tables 3 and 4), and the log-linear regression model provided the best fit.

In newborns, FA was highest in splenium followed by the genu of the corpus callosum, MCP, PLIC, SCP, and ICP (Fig. 2). The highest increase in FA in cerebral white matter was observed up to the age of 24 months, while in cerebellar white matter, it was up to 36 months followed by a gradual continuous rise subsequently in both cerebral and cerebellar white matter (Fig. 2). However, the degree of increase in FA was higher in cerebellar white matter compared to cerebral white matter. At the end of

Table 1 Relationship between age and fractional anisotropy (FA) in cerebral and cerebellar white matter of the developing brain using log-linear regression model

Regions	FA (Mean ± SD)	Regression coefficients		Model diagnostics			95% CI of mean	
		b_0	b_1	R^2	F	Significance	Lower	Upper
Splenium of CC	0.48±0.04	0.4224	0.0208	0.878	136.32	0.000	0.46	0.50
Genu of CC	0.47±0.04	0.4193	0.0185	0.900	170.93	0.000	0.45	0.48
PLIC	0.38±0.03	0.3453	0.0145	0.642	71.82	0.000	0.37	0.39
MCP	0.45±0.06	0.3699	0.0316	0.920	458.68	0.000	0.43	0.47
SCP	0.35±0.06	0.2724	0.0306	0.969	1243.57	0.000	0.33	0.37
ICP	0.34±0.05	0.2721	0.0272	0.905	380.96	0.000	0.33	0.36

CC corpus callosum, PLIC posterior limb of the internal capsule, MCP middle cerebellar peduncles, SCP superior cerebellar peduncles, ICP inferior cerebellar peduncles, CI confidence interval

132 months, the splenium of corpus callosum still showed highest FA, followed by the MCP, genu of the corpus callosum, SCP, PLIC, and ICP (Fig. 2).

The MD was highest in the genu of the corpus callosum followed by the PLIC, splenium of the corpus callosum, ICP, SCP, and MCP during the early period (Fig. 3). The MD showed an initial sharp decrease in cerebral white matter up to the age of 24 months, while in the cerebellar white matter, it was observed up to 6 months (Fig. 3). In cerebral white matter after 24 months, the MD showed a decreased pattern (Fig. 3). However, in cerebellar white matter, an initial decrease (6 months) in MD was noticed, which later stabilized (Fig. 3). After 132 months, the genu of the corpus callosum showed highest MD followed by the splenium of the corpus callosum, PLIC, ICP, SCP, and MCP (Fig. 3).

Discussion

This study demonstrates the potential of DTI indices (FA and MD) in assessment of cerebral (splenium and genu of the corpus callosum and PLIC) and cerebellar (MCP, SCP, and ICP) white matter maturation with the progression of

age. In the current study, the log-linear model showed best fit to describe the age-related changes in the DTI indices (FA and MD) both for cerebral and cerebellar white matter. The pattern of log-linear graphs showed that in cerebral white matter, an initial sharp increase in FA was observed up to the age of 24 months followed by a gradual increase up to 132 months. In cerebellar white matter, sharp increase in FA was observed up to 36 months, which then followed a gradual increase. On the other hand, MD showed a sharp decrease in cerebral white matter up to 24 months followed by a more gentle decrease thereafter, while in cerebellar white matter, after initial decrease (6 months), it followed a stable pattern.

Previous studies have shown that in neonates, as the brain matures, there is a gradual increase in FA and decrease in MD in the white matter, and this is believed to be associated with the process of myelination [17, 26–28]. All these studies have described age-related changes in DTI indices in cerebral white matter. As far as we know, there is no study till date that describes the changes in DTI indices as a function of age in cerebellar white matter. Morriss et al. [17] demonstrated changes in ADC and FA during the first 3 years of life in major white matter tracts in children aged between 1 day to 17 years. Schneider et al.

Table 2 Relationship between age and mean diffusivity (MD; 10^{-3} mm²/s) in cerebral and cerebellar white matter of the developing brain using log-linear regression model

Regions	MD (Mean ± SD)	Regression coefficients		Model diagnostics			95% CI of mean	
		B_0	b_1	R^2	F	Significance	Lower	Upper
Splenium of CC	1.00±0.16	1.1929	−0.0753	0.857	113.72	0.000	0.93	1.07
Genu of CC	1.09±0.22	1.3682	−0.1090	0.885	146.30	0.000	0.98	1.18
PLIC	1.00±0.19	1.2416	−0.0954	0.942	651.32	0.000	0.94	1.05
MCP	0.66±0.03	0.6971	−0.0151	0.809	169.16	0.000	0.65	0.67
SCP	0.67±0.03	0.7143	−0.0166	0.848	222.84	0.000	0.66	0.68
ICP	0.71±0.05	0.7734	−0.0238	0.901	363.38	0.000	0.70	0.73

CC corpus callosum, PLIC posterior limb of the internal capsule, MCP middle cerebellar peduncles, SCP superior cerebellar peduncles, ICP inferior cerebellar peduncles, CI confidence interval

Table 3 Fractional anisotropy (mean \pm SD) values in different cerebral and cerebellar white matter regions of children in different age groups

Regions	Age (months)			
	0.2–3.5 months	8–12 months	15–24 months	48–132 months
Splenium of CC	0.42 \pm 0.01	0.48 \pm 0.01	0.49 \pm 0.01	0.52 \pm 0.02
Genu of CC	0.42 \pm 0.03	0.47 \pm 0.02	0.49 \pm 0.01	0.49 \pm 0.01
PLIC	0.35 \pm 0.02	0.37 \pm 0.01	0.37 \pm 0.02	0.42 \pm 0.03
MCP	0.37 \pm 0.05	0.44 \pm 0.03	0.47 \pm 0.02	0.51 \pm 0.01
SCP	0.27 \pm 0.04	0.34 \pm 0.02	0.38 \pm 0.01	0.40 \pm 0.01
ICP	0.27 \pm 0.05	0.34 \pm 0.02	0.37 \pm 0.01	0.38 \pm 0.02

CC corpus callosum, PLIC posterior limb of the internal capsule, MCP middle cerebellar peduncles, SCP superior cerebellar peduncles, ICP inferior cerebellar peduncles

[28] performed DTI study in 52 children ranging from 1 day to 16 years and found an increased FA and decreased isotropic diffusion with age in cerebral white matter. They showed that monoexponential regression function was found to be the best fit to describe the age-related changes in FA and isotropic diffusion for the splenium and genu of the corpus callosum [28]. Mukherjee et al. [26] demonstrated that age-related increase in anisotropy and reduction in ADC in 153 children ranging from 1 day to 11 years followed a biexponential model in the splenium of the corpus callosum and internal capsule except for monoexponential regression in the genu of the corpus callosum. They observed large and fast early rise in anisotropy during the first 2 years of postnatal life followed by a slower growth subsequently. This time course paralleled the maturational decline in water diffusion followed by slower decay of ADC [26]. They suggested that these changes are most likely due to the progression of myelination in central white matter tracts [26].

In the current study, swift increase in FA was observed in cerebral white matter during the first 24 months and is consistent with the previous findings [26, 28, 29]. However, swift rise in FA was observed during the first 36 months in cerebellar white matter in the current study. This difference in the duration in the white matter maturation between

cerebral and cerebellar white matter suggests that cerebellar white matter myelination takes much longer to complete as compared to cerebral white matter. The progressive slower increase in FA both in cerebral and cerebellar white matter subsequently up to the age of 132 months suggests continuing myelination, increased organization, and compactness of the axonal bundles. These results are consistent with previous studies, which showed that the rate of myelination slows after 2 years of age [38] and continues during childhood and adolescence [39].

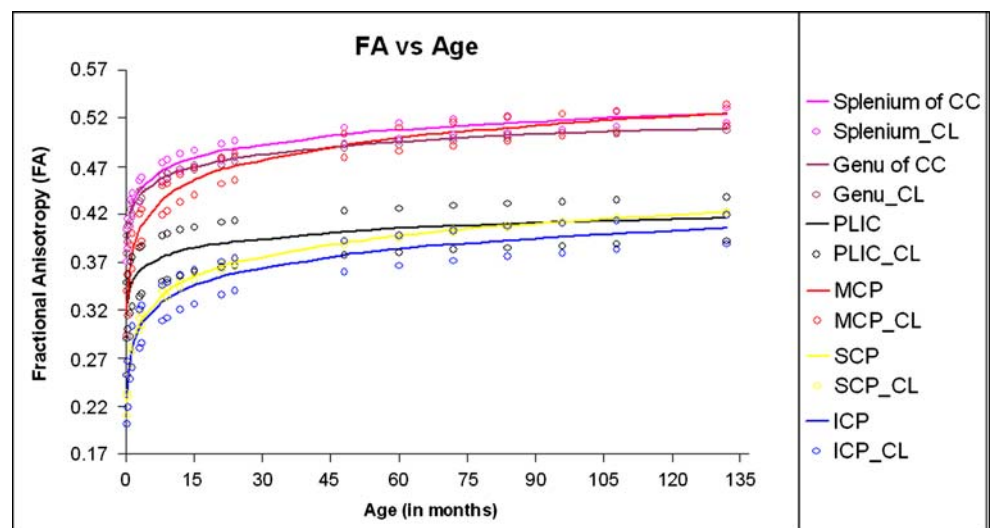
It has been reported that the age-dependent decline in MD parallels the rise in FA in major white matter tracts [26, 28]. In the current study, the pattern of MD was also described by the log-linear regression model both in cerebral and cerebellar white matter. Mukherjee et al. [26] demonstrated large and rapid early maturational decline in ADC during the first 2 years of postnatal life, and a smaller and slower late decay of ADC predominating thereafter. This maturational time course of ADC closely paralleled that of changes in brain water content with age, although the 46% drop in ADC between term birth and adulthood was much larger than the 12% decrease in brain water content over that interval as determined from brain specimens [40]. Hence, the age-dependent reduction of MD reflects more than just tissue water loss. During develop-

Table 4 Mean diffusivity ($\times 10^{-3}$ mm²/s; mean \pm SD) values in different cerebral and cerebellar white matter regions of children in different age groups

Regions	Age (months)			
	0.2–3.5 months	8–12 months	15–24 months	48–132 months
Splenium of CC	1.22 \pm 0.08	0.99 \pm 0.03	0.93 \pm 0.03	0.87 \pm 0.02
Genu of CC	1.36 \pm 0.05	1.23 \pm 0.04	1.01 \pm 0.07	0.86 \pm 0.05
PLIC	1.24 \pm 0.09	1.08 \pm 0.08	0.91 \pm 0.06	0.82 \pm 0.03
MCP	0.69 \pm 0.04	0.66 \pm 0.00	0.65 \pm 0.01	0.63 \pm 0.01
SCP	0.71 \pm 0.02	0.69 \pm 0.01	0.66 \pm 0.01	0.64 \pm 0.01
ICP	0.77 \pm 0.03	0.72 \pm 0.01	0.71 \pm 0.03	0.66 \pm 0.01

CC corpus callosum, PLIC posterior limb of the internal capsule, MCP middle cerebellar peduncles, SCP superior cerebellar peduncles, ICP inferior cerebellar peduncles

Fig. 2. Relationship between fractional anisotropy (FA) and age in different cerebral and cerebellar white matter regions of children ranging in age from birth to 132 months. *CC* corpus callosum, *PLIC* posterior limb of the internal capsule, *MCP* middle cerebellar peduncles, *SCP* superior cerebellar peduncles, *ICP* inferior cerebellar peduncles, *CL* confidence limit

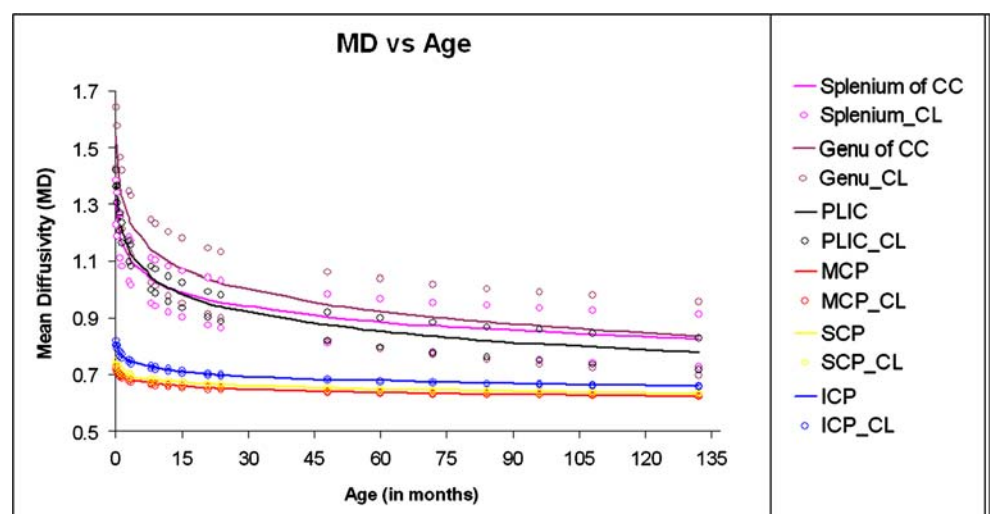


ment, other factors that influence MD include increased binding of water to macromolecules such as myelin, reducing free water content, and the formation of new structural barriers to water diffusion such as dendritic arborization, axonal ramification, synaptogenesis, and glial proliferation within gray matter as well as progressive myelination within white matter [13]. In the current study, the fast decline in MD was observed up to the age of 24 months in cerebral white matter thereafter becoming gradual in keeping with the log-linear decline. The fast decline in the MD component may be linked to the decreasing amount of extracellular space and/or increasing concentration of intracellular macromolecules [41]. Furthermore, the gradual decrease in MD might be due to the ongoing reduction in the total water content of the brain, which decreases by 14–18% from birth to adulthood [40]. However, the cerebellar white matter showed fast log-linear decrease in MD compared to cerebral white matter. In

cerebellar white matter, the fast log-linear decrease in MD component was observed up to the period of 6 months and then tended toward stabilization. It has been reported that the cerebellar white matter loses its water relatively rapidly compared to other parts of the brain [42]. We speculate that this may be the possible reason for the fast decrease in MD in cerebellar white matter compared to cerebral white matter. No further change in MD suggests that there might have been no significant reduction in water content subsequently. The pattern of log-linear regression graph for these two indices (FA and MD) showed that FA provides more accurate information in assessing the white matter maturation (cerebral and cerebellar white matter) compared to MD.

In a number of cerebellar conditions like spino-cerebellar degeneration, cerebellar cognitive affective syndrome, and cerebellar motor syndrome, conventional imaging may or may not show much abnormality [43]. This study may provide a normative data of cerebellar peduncles that might

Fig. 3. Relationship between mean diffusivity (MD; $10^{-3} \text{ mm}^2/\text{s}$) and age in different cerebral and cerebellar white matter regions of children ranging in age from birth to 132 months. *CC* corpus callosum, *PLIC* posterior limb of the internal capsule, *MCP* middle cerebellar peduncles, *SCP* superior cerebellar peduncles, *ICP* inferior cerebellar peduncles, *CL* confidence limit



be of value in identifying the abnormality in cerebellar white matter on DTI. This baseline information may aid the neuroradiologists in differentiating normal from abnormal white matter.

Conclusion

We conclude that changes in the magnitude and anisotropy of water diffusion follow different time courses during cerebral and cerebellar white matter development that may be described with a log-linear regression model. This study might provide a normative database of brain white matter development from neonates to childhood. This information may be useful for assessing brain maturation in patients with developmental delay associated with cerebral and cerebellar white matter.

Acknowledgment This study was supported by grant no. BT/PR5009/Med/14/581/2004 from the Department of Biotechnology, New Delhi, India. Sona Saksena acknowledges the financial assistance from the Indian Council of Medical Research, New Delhi, India. Richa Trivedi acknowledges the financial assistance from the Council of Scientific and Industrial Research, New Delhi, India.

References

1. Yakovlev PI, Lecours AR (1967) The myelogenetic cycles of regional maturation of the brain. In: Minkowski A (ed) *Regional development of the brain in early life*. Oxford, England, Blackwell Scientific, pp 3–70
2. Ricardson EP Jr (1982) Myelination in the human central nervous system. In: Haymaker W, Adams RD (eds) *Histology and histopathology of the nervous system*. Springfield, III, Thomas, pp 146–73
3. Barkovich AJ (2000) Concepts of myelin and myelination in neuroradiology. *AJNR Am J Neuroradiol* 21:1099–1109
4. Paus T, Collins DL, Evans AC, Leonard G, Pike B, Zijdenbos A (2001) Maturation of white matter in the human brain: a review of magnetic resonance studies. *Brain Res Bull* 54:255–266
5. Schmithorst VJ, Wilke M, Dardzinski BJ, Holland SK (2005) Cognitive functions correlate with white matter architecture in a normal pediatric population: a diffusion tensor MRI study. *Hum Brain Mapp* 26:139–147
6. Paus T, Zijdenbos A, Worsley K, Collins L, Blumenthal J, Giedd JN et al (1999) Structural maturation of neural pathways in children and adolescents: in vivo study. *Science* 283:1908–1911
7. Brody BA, Kinney HC, Kloman AS, Gilles FH (1987) Sequence of central nervous system myelination in human infancy. I. An autopsy study of myelination. *J Neuropathol Exp Neurol* 46:283–301
8. Kinney HC, Brody BA, Kloman AS, Gilles FH (1988) Sequence of central nervous system myelination in human infancy. II. Patterns of myelination in autopsied infants. *J Neuropathol Exp Neurol* 47:217–234
9. Gilles FH, Shankle W, Dooling EC (1983) Myelinated tracts: growth patterns. In: Gilles FH, Leviton A, Dooling EC (eds) *The developing human brain*. PSG, Boston, John Wright, pp 117–183
10. Barkovich AJ, Kjos BO, Jackson DE Jr, Norman D (1988) Normal maturation of the neonatal and infant brain: MR imaging at 1.5 T. *Radiology* 166:173–180
11. van der Knaap MS, Valk J (1990) MR imaging of the various stages of normal myelination during the first year of life. *Neuroradiology* 31:459–470
12. Barkovich AJ (ed) (2005) *Pediatric neuroimaging*, 4th edn. Lippincott, Philadelphia
13. Mukherjee P, McKinstry RC (2006) Diffusion tensor imaging and tractography of human brain development. *Neuroimaging Clin N Am* 16:19–43
14. Wimberger DM, Roberts TP, Barkovich AJ, Prayer LM, Moseley ME, Kucharczyk J (1995) Identification of “premyelination” by diffusion-weighted MRI. *J Comput Assist Tomogr* 19:28–33
15. Prayer D, Barkovich AJ, Kirschner DA, Prayer LM, Roberts TP, Kucharczyk J et al (2001) Visualization of nonstructural changes in early white matter development on diffusion-weighted MR images: evidence supporting premyelination anisotropy. *AJNR Am J Neuroradiol* 22:1572–1576
16. Nomura Y, Sakuma H, Takeda K, Tagami T, Okuda Y, Nakagawa T (1994) Diffusional anisotropy of the human brain assessed with diffusion-weighted MR: relation with normal brain development and aging. *AJNR Am J Neuroradiol* 15:231–238
17. Morriss MC, Zimmerman RA, Bilaniuk LT, Hunter JV, Haselgrove JC (1999) Changes in brain water diffusion during childhood. *Neuroradiology* 41:929–934
18. Kizildağ B, Düşünceli E, Fitoz S, Erden I (2005) The role of classic spin echo and FLAIR sequences for the evaluation of myelination in MR imaging. *Diagn Interv Radiol* 11:130–136
19. Murakami JW, Weinberger E, Shaw DW (1999) Normal myelination of the pediatric brain imaged with fluid-attenuated inversion-recovery (FLAIR) MR imaging. *AJNR Am J Neuroradiol* 20:1406–1411
20. Engelbrecht V, Rassek M, Preiss S, Wald C, Modder U (1998) Age-dependent changes in magnetization transfer contrast of white matter in the pediatric brain. *AJNR Am J Neuroradiol* 19:1923–1929
21. van Buchem MA, Steens SC, Vrooman HA, Zwinderman AH, McGowan JC, Rassek M et al (2001) Global estimation of myelination in the developing brain on the basis of magnetization transfer imaging: a preliminary study. *AJNR Am J Neuroradiol* 22:762–766
22. Beaulieu C (2002) The basis of anisotropic water diffusion in the nervous system—a technical review. *NMR Biomed* 15:435–455
23. Neil JJ, Shiran SI, McKinstry RC, Schefft GL, Snyder AZ, Almlı CE et al (1998) Normal brain in human newborns: apparent diffusion coefficient and diffusion anisotropy measured by using diffusion tensor MR imaging. *Radiology* 209:57–66
24. Huppi PS, Maier SE, Peled S, Zientara GP, Barnes PD, Jolesz FA et al (1998) Microstructural development of human newborn cerebral white matter assessed in vivo by diffusion tensor magnetic resonance imaging. *Pediatr Res* 44:584–590
25. McKinstry RC, Mathur A, Miller JH, Ozcan A, Snyder AZ, Schefft GL et al (2002) Radial organization of developing preterm human cerebral cortex revealed by non-invasive water diffusion anisotropy MRI. *Cereb Cortex* 12:1237–1243
26. Mukherjee P, Miller JH, Shimony JS, Conturo TE, Lee BC, Almlı CR et al (2001) Normal brain maturation during childhood: developmental trends characterized with diffusion-tensor MR imaging. *Radiology* 221:349–358

27. McGraw P, Liang L, Provenzale JM (2002) Evaluation of normal age-related changes in anisotropy during infancy and childhood as shown by diffusion tensor imaging. *AJR Am J Roentgenol* 179:1515–1522
28. Schneider JF, Il'yasov KA, Hennig J, Martin E (2004) Fast quantitative diffusion-tensor imaging of cerebral white matter from the neonatal period to adolescence. *Neuroradiology* 46: 258–266
29. Hermoye L, Saint-Martin C, Cosnard G, Lee SK, Kim J, Nassogne MC et al (2006) Pediatric diffusion tensor imaging: normal database and observation of the white matter maturation in early childhood. *Neuroimage* 29:493–504
30. Dubois J, Hertz-Pannier L, Dehaene-Lambertz G, Cointepas Y, Le Bihan D (2006) Assessment of the early organization and maturation of infants' cerebral white matter fiber bundles: a feasibility study using quantitative diffusion tensor imaging and tractography. *Neuroimage* 30:1121–1132
31. Le Bihan D (ed) (1995) *Diffusion and perfusion MRI—applications to functional MRI*. Raven, New York
32. Hasan KM, Parker DL, Alexander AL (2001) Comparison of gradient encoding schemes for diffusion-tensor MRI. *J Magn Reson Imaging* 13:769–780
33. Woods RP, Mazziotta JC, Cherry SR (1993) MRI–PET registration with automated algorithm. *J Comput Assist Tomogr* 17: 536–546
34. Purwar A, Gupta RK, Sarma MK, Bayu G, Singh A, Rathore DK et al (2006) De-scalping of the brain in echo planar DT-MRI. *Proceedings of the International Society of Magnetic Resonance in Medicine*, p 325
35. Hasan KM, Basser PJ, Parker DL, Alexander AL (2001) Analytical computation of the eigenvalues and eigenvectors in DT-MRI. *J Magn Reson* 152:41–47
36. Purwar A, Rathore DK, Rathore RKS, Gupta RK (2006) A DTI analysis tool. *Proceedings of the European Society of Magnetic Resonance in Medicine*, Abstract 644
37. Wakana S, Jiang H, Nagae-Poetscher LM, van Zijl PC, Mori S (2004) Fiber tract-based atlas of human white matter anatomy. *Radiology* 230:77–87
38. Dietrich RB, Bradley WG, Zaragoza EJ IV, Otto RJ, Taira RK, Wilson GH et al (1988) MR evaluation of early myelination patterns in normal and developmentally delayed infants. *AJR Am J Roentgenol* 150:889–896
39. Benes FM, Turtle M, Khan Y, Farol P (1994) Myelination of a key relay zone in the hippocampal formation occurs in the human brain during childhood, adolescence, and adulthood. *Arch Gen Psychiatry* 51:477–484
40. Dobbing J, Sands J (1973) Quantitative growth and development of human brain. *Arch Dis Child* 48:757–767
41. Engelbrecht V, Scherer A, Rassek M, Witsack HJ, Mödder U (2002) Diffusion-weighted MR imaging in the brain in children: findings in the normal brain and in the brain with white matter diseases. *Radiology* 222:410–418
42. Stricker T, Martin E, Boesch C (1990) Development of the human cerebellum observed with high-field-strength MR imaging. *Radiology* 177:431–435
43. Schmahmann JD (2004) Disorders of the cerebellum: ataxia, dysmetria of thought, and the cerebellar cognitive affective syndrome. *J Neuropsychiatry Clin Neurosci* 16:367–378